ELSEVIER

Cement & Concrete Composites 25 (2003) 97–108

Cement & Concrete Composites

www.elsevier.com/locate/cemconcomp

Porosity of cement paste cured at 45 °C as a function of location relative to casting position

J.M. Khatib *, P.S. Mangat

School of Environment and Development, Sheffield Hallam University, Howard Street, Sheffield S1 1WB, UK

Received 16 March 2001; accepted 6 December 2001

Abstract

The influence of location relative to the casting position, on porosity and pore size distribution of cement pastes, was investigated. Three different pastes were prepared at a constant water/binder ratio of 0.45. The pastes were the control paste (CP) in which Portland cement was used and no cement replacement materials were added, pastes with 22% and 9% replacement (by mass) of cement with fly ash (FA) and silica fume (SF), respectively. Paste specimens were cast in cube moulds and were either cured in air at a temperature of 45 °C and relative humidity of 25% for 28 days or moist cured for 14 days after casting at 45 °C, followed by air curing at 45 °C and 25% relative humidity for further 14 days. Samples were taken from various locations of the cube specimens. Porosity and pore size distribution were conducted on the paste samples using the mercury intrusion porosimetry technique.

The results show that large differences in porosity and pore size distribution exist between samples taken from different locations relative to casting positions. These differences are larger in pastes subjected to dry curing as compared to pastes subjected to some initial moist curing. The influence of sample location relative to casting position on porosity and pore size distribution of paste is compared with absorption of concrete performed in a previous investigation. The correlation between pore volume of paste and water absorption of concrete is also conducted.

Keywords: Curing; Fly ash; High temperature; Intruded pore volume; Location; Pore size distribution; Silica fume

1. Introduction

There is a wealth of information in the literature related to porosity and pore size distribution of cement paste [1–21]. However there is little work on quantifying the influence of location of sample within the paste matrix relative to the casting position on porosity and pore size distribution. Owing to the bleeding effect of cement or cementitious materials when water is present and which occurs during the early stages after casting, the porosity and pore size distribution is expected to vary between the top (trowelled) layer and the other layers of the paste or concrete. Bleeding describes the upward movement of water to the freshly placed paste or concrete resulting from the settlement of heavier solid particles [22–25]. The bleeding results in a variation in the effective water content throughout the various zones of concrete or paste matrix, which produces corresponding changes in their properties. These properties include porosity, pore size distribution and strength.

Bleeding in concrete is also influenced by the presence of pozzolanic materials. Generally, it is accepted that the bleeding is reduced when fly ash (FA) or silica fume (SF) are used in concrete [26,27]. This is partly due to the smoother particle shape of the FA particles, and due to the ultra-fine particles of the silica fume resulting in a more cohesive concrete [26,27].

Also the concrete or paste properties are expected to vary between the side surface, which is exposed to the external environment, and the middle core of specimens. The lack of moisture results in restricted hydration and affects the porosity and pore size distribution of the paste or concrete. Therefore dry curing leads to a high porosity and a coarser pore size distribution of paste compared to specimens provided initially with some moist curing [10,12,18].

It is well established that the incorporation of pozzolanic materials such as FA or SF affects the porosity

* Corresponding author. Fax: +44-0-114-225-4546.
E-mail address: j.m.khatib@shu.ac.uk (J.M. Khatib).

0958-9465/03/$ - see front matter
PII: S0958-9465(01)00093-2

and pore size distribution of cement paste. At normal curing temperature, the partial substitution between 10% and 70% (by mass) of cement with FA is reported to increase the porosity and pore size of the paste during the early stages of hydration [18,21,28,29] and up to a curing period of 28 days. As hydration continues beyond 28 days this effect is much reduced as more additional calcium silicate hydrate gel is formed and therefore the presence of FA in a cement paste is beneficial [21,28,29]. The incorporation of SF is reported to positively contribute to the short and long term properties of paste or concrete. These properties include strength and porosity [29]. Other workers [3,7,12] reported that the presence of SF increases the pore volume of paste or mortars containing relatively a high water content and subjected to inadequate initial curing. However, the strength is found to increase regardless of the curing method adopted [12].

Strength and porosity of paste or concrete are related and many equations are suggested to describe this relationship [5,13,17,19,21]. Generally, an increase in porosity results in a decrease in strength. Porosity is mainly influenced by the strength properties of the paste regardless of the water to cement ratio or the degree of the hydration [5]. Others [17] reported that relationship between porosity and compressive strength of the paste is affected by the water to cement ratio. The relationship in the early stages of hydration is controlled by maximum pore size, whereas in the later stage it is controlled by the porosity [5,17,21]. Strength of paste is found to be more heavily influenced by the porosity, the percentage of large pores and the mean pore diameter than the amount of small pores [19,21]. In addition to the dependency of strength on porosity and pore size distribution, the morphology of the hydrated products influences the strength and thereby the relationship between strength and porosity [19].

The influence of location on porosity of concrete as indicated by water absorption and capillary rise is discussed elsewhere [14]. The amount of bleeding in concrete is different than that of pastes, owing to the presence of aggregates in the former. This paper attempts to determine the porosity and pore size distribution of samples taken from various locations of paste specimens. Specimens were subjected to high temperature curing to simulate curing in hot weather. The materials considered are pastes based on Portland cement and pastes in which cement was partially replaced with FA or SF. The influence of sample location on the porosity of paste is compared with that of absorption of concrete reported in a previous work on specimens of the same size [14]. A correlation between the porosity of paste, absorption and strength of concrete is presented.

2. Experimental

2.1. Mix proportions and materials

Three different pastes were used to study the influence of varying the location of samples relative to the casting position on porosity and pore size distribution, details of which are given in Table 1. The pastes were the control paste (CP) in which ordinary Portland cement was used. In the fly ash paste (FAP) and silica fume paste (SFP), the cement was partially replaced (by mass) with, respectively, 22% FA and 9% SF. The water/binder ratio was kept constant at 0.45. Binder consisted of cement and cement replacement materials. Superplasticizer (SP), which conforms to types F and G material, of ASTM-C494, was added to all pastes. The dosage of SP was 1.2% by mass of binder for the CP and the FAP whereas 1.5% was added to the SFP.

Cubes of 100 mm side were cast from three concrete mixes. These were used for the determination of compressive strength. The mixes proportions by mass were 1 (binder):2 (fine aggregates):3.4 (coarse aggregates). The binder compositions, the water to binder ratio and the SP content of the concrete mixes were identical to the three pastes. The slump of the concrete mixes ranged from 80 to 105 mm. The concrete containing SF contained larger dosage of SP (i.e., 1.5%) to compensate for the loss in workability.

The composition of cement and cement replacement materials is given elsewhere [30].

2.2. Specimen preparation and curing

The dry materials of the pastes were placed in a food mixer and blended for about 2 min until a uniform colour was obtained. This was followed by the slow addition of water. Mixing was then continued until uniform paste was achieved. Paste specimens in the form of cubes of 100 mm side were cast in steel moulds and compacted using a vibrating table for a few seconds. The large size paste specimens were used, so that comparison can be made between the results on pore volume of paste of this work and results on water absorption of concrete reported in a previous investigation made with specimens of the same size [14]. The purpose of the present investigation was to study the difference in porosity and pore size distribution for samples taken from various locations relative to casting position and, therefore, paste specimens were not rotated after casting. One cube was cast for each of the two curing methods used in this investigation. The temperature and relative humidity during casting are presented in Table 2 and outlined below:

(a) After casting, specimens in the moulds were kept in a controlled environmental chamber where the tem-

Table 1
Details of paste mixes

Paste	Paste code	Proportions (% by mass of binder)			
		Cement	Fly ash	Silica fume	SP[a]
Control	CP	100	0	0	1.2
Fly ash	FAP	78	22	0	1.2
Silica fume	SFP	91	0	9	1.5

[a] Superplasticizer.

Table 2
Details of curing methods

Curing (code)	After casting and before demoulding	After demoulding	
	Up to 24 h	After 24 h and up to 14 days	After 14 days and up to 28 days
Air (A)	Exposed to air at 45 °C & 25% RH	Exposed to air at 45 °C & 25% RH	Exposed to air at 45 °C & 25% RH
Wet-air (WA)	Covered with plastic sheeting and wet burlap at 45 °C & 25%RH	Covered with plastic sheeting and wet burlap at 45 °C & 25%RH	Exposed to air at 45 °C & 25% RH

perature was 45 °C and relative humidity (RH) was 25% for a period of 24 h. The top surface of the specimens was left exposed while in the moulds. After 24 h the specimens were demoulded and left exposed in the chamber for a further 27 days. Specimens were designated as A and are called air cured.

(b) Soon after casting, the specimens were placed in the controlled chamber at 45 °C and 25% RH and were covered with plastic sheeting and wet burlap. After 24 h, the specimens were demoulded and immediately re-covered with wet burlap and plastic sheeting and remained in this chamber for 13 days. The burlap was kept wet during the first 14 days. After 14 days from casting, the covers were removed and specimens were left exposed to air at 45 °C, 25% RH for a further 14 days. The specimens were designated as WA and they are called wet-air cured.

For strength determination concrete specimens were cured in the same way as in (a) and (b) apart from the curing temperature which was 37 °C instead of 45 °C. The concrete strength determination formed part of another study, and that is why the temperature of curing was not the same.

2.3. Sampling of paste

Each cube specimen was crushed and solid samples for testing were taken from various locations of the cube as shown in Fig. 1. The mass of each sample ranged between 0.8 and 2.5 g. The different positions are described as follows:

(a) *Position 1*. Samples were taken from the middle of the top (trowelled) face and were designated as T for top.

(b) *Position 2*. Samples were taken from the middle of the bottom face, which is opposite to the top face and were designated as B for bottom.

(c) *Position 3*. Samples were taken from the middle (core) of the cube and were designated as MI for middle.

(d) *Position 4*. Samples were taken from the middle of the side (cast) face and were designated as S for side.

After collection, paste samples were placed in an oven at 100 ± 5 °C until a constant mass was achieved. This normally took 24 h. The samples were then placed in an air tight container until the time of testing. The influence of this drying method (i.e., 100 °C) on the possible alterations of pore structure was not investigated.

2.4. Testing

Mercury intrusion porosimetry technique was employed to measure the porosity and pore size distribution

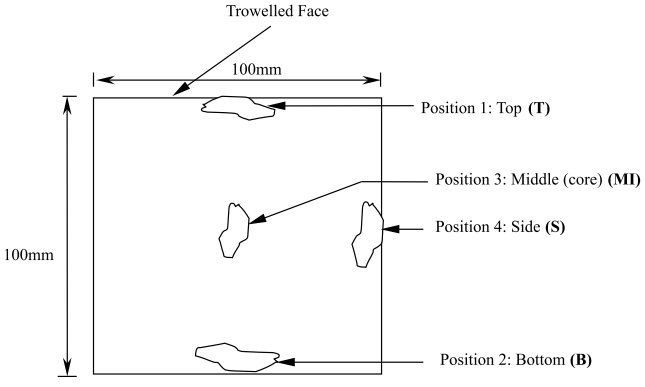

Fig. 1. Locations of samples for MIP test (section through vertically cast cube).

of the samples. One sample per location was tested. The apparatus has a 200 MPa pressure capacity. The data were computed using the following Washburn equation [31]:

$$D = -\frac{4\delta\cos\phi}{P},$$

where D is the pore diameter in μm, P is the applied pressure in kPa, δ is the surface tension which was taken as 484 dynes/cm and ϕ is the contact angle which was taken as 142°.

3. Results and discussion

3.1. Intruded pore volume

The intruded pore volume of pastes, CP, FAP and SFP exposed to air curing and wet-air curing is presented in Fig. 2 for the various locations considered. Generally and as can be expected, the results indicate that samples taken from the top position possess the largest intruded pore volume, followed by respectively the samples taken from the side, middle and bottom positions.

In the CP and under air curing, there is an increase of over 80% in the intruded pore volume for the sample taken from the top position as compared to that taken from the bottom position. The increase in the intruded pore volume is much lower (45%) in the FAP, which shows that the presence of FA in the paste seems to have a beneficial effect on bleeding.

The influence of initial curing on the intruded pore volume of samples taken from the top and bottom position is also apparent in Fig. 2. Specimens subjected to wet-air curing possess lower pore volumes as compared with those subjected to air curing for samples taken from the various locations (i.e., T, S, MI and B). More detailed results on the influence of initial curing and replacement materials on intruded pore volume are reported elsewhere [10]. The difference in intruded pore volume between samples taken from the top face and the bottom is much less in pastes subjected to some wet-air curing. A difference of 50% is observed in the CP under such a curing as compared to 80% under air curing. This indicates that under more favourable moist curing, a greater degree of hydration of the more porous zone narrows the difference in pore volume in different zones.

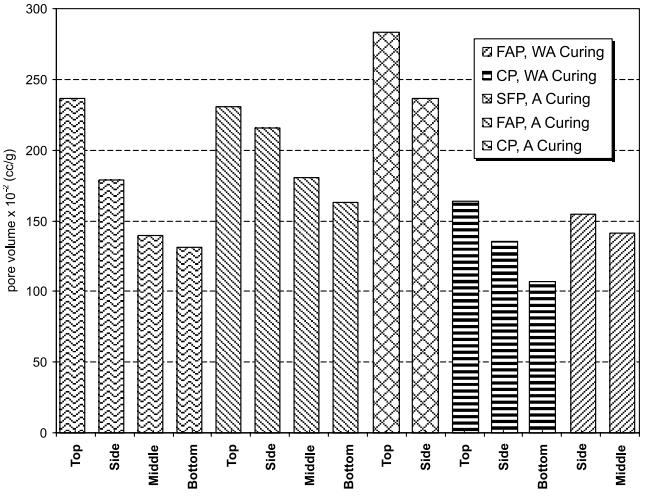

Fig. 2. Influence of location on intruded pore volume for the various pastes.

Under air curing, the intruded pore volume for samples taken from the side surface of the cube is higher than that of samples taken from the middle core. The variation is slightly less in the case of FAP. The difference in intruded pore volume for samples taken from the middle and the side is considerably less in specimens subjected to wet-air curing as compared to those subjected to air curing. The availability of water under wet-air curing allows more hydration to take place, and subsequently less pore volume is obtained in samples taken from the side position for pastes subjected to such a curing, as compared with those subjected to dry curing.

The SFP possesses larger pore volume than the CP and the FAP, for samples taken from both the top and side positions and subjected to air curing. Due to the rapid loss of water under such a curing, the SF particles did not develop sufficient hydration products to form further calcium silicate hydrate gel. This is in agreement with results obtained elsewhere [3,10,12].

3.2. Pore size distribution

The pore size distribution for the CP subjected to air curing for samples taken from various locations of the paste matrix (i.e., cubes) is shown in Fig. 3. It can be noticed that the dominant pore size of the top surface is far larger than any other locations. The dominant pore size, however, is the pore diameter on the incremental pore volume plot at which the maximum value of incremental volume is obtained. The dominant pore size of the top surface is 1.5 μm whereas a value of 0.2 μm is obtained for the bottom surface. The dominant pore size of the side surface and the middle part (core) is similar to that of the bottom surface. Similar trend is obtained on the influence of sample position on dominant pore size for FAP under air curing as shown in Fig. 4.

The pore size distribution of the SFP for the top and the side positions of specimens exposed to air curing is presented in Fig. 5. The trend is somewhat different in that the dominant pore size for both positions is similar at about 0.15 μm in diameter.

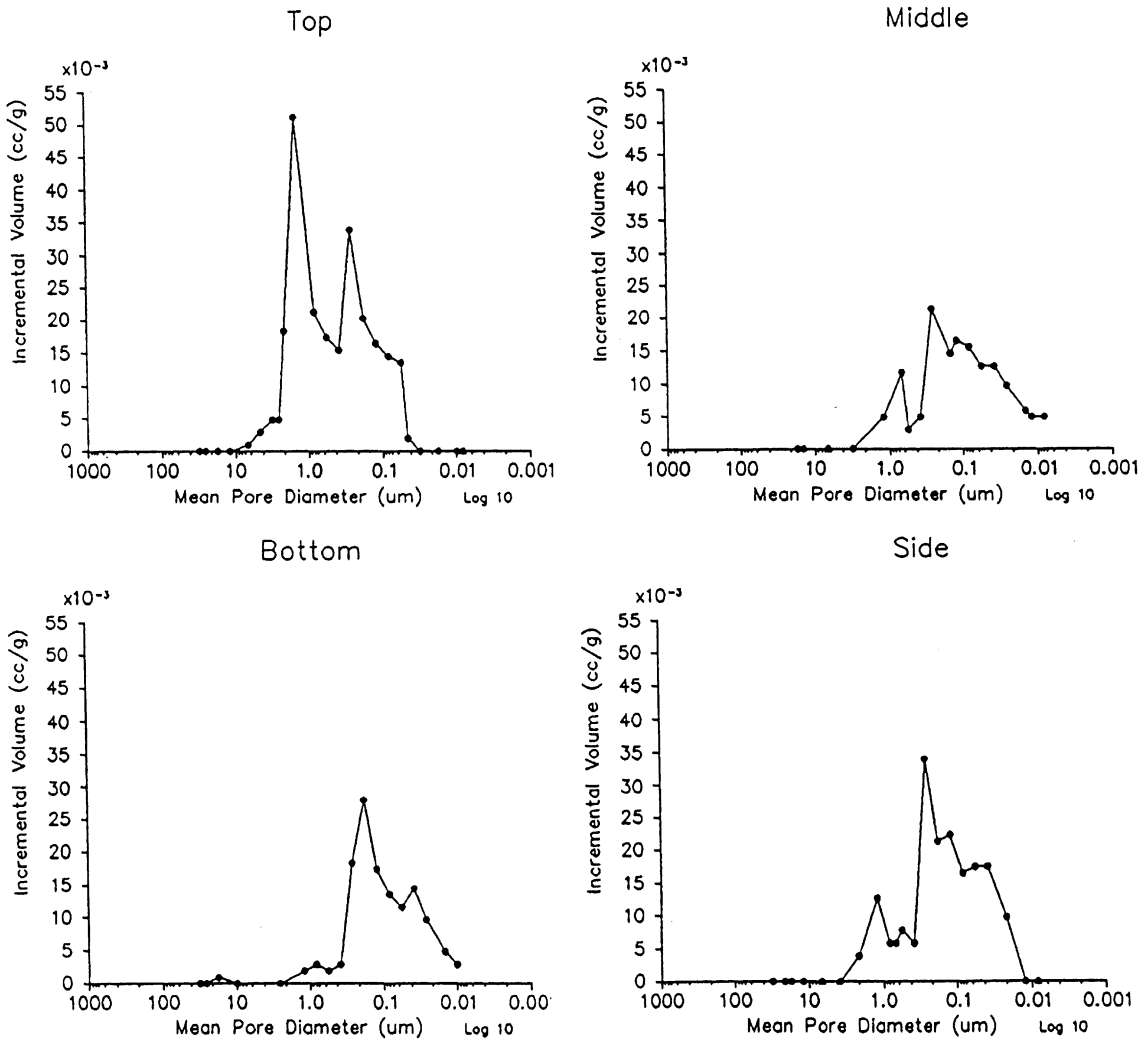

Fig. 3. Influence of position on pore size distribution for the CP subjected to air curing.

Wet-air cured specimens on the other hand, behaved differently. This is shown in Fig. 6, where the pore size distribution of samples taken from different positions under such curing is presented for the control paste. The dominant pore sizes for the top, bottom and the side faces are similar at about 0.15 μm. This is due to the availability of water at the top face of the paste during the first 14 days of curing, which results in greater hydration of cement and therefore, pores were filled with the products of hydration. In Fig. 7, where the incremental pore volume for the FAP is presented under wet-air curing for the middle and the side position, the dominant pore size for the side surface is larger than that of the middle position. This might be explained by the fact that FA particles take longer time than cement to hydrate. After 14 days of initial moist curing, specimens were subjected to air curing for 14 more days, and therefore, the availability of water on the side surface is less than that in the middle core, which might limit the hydration of FA particles.

The durability of paste is not only dependent on its porosity and the dominant pore size, it is also dependent on its threshold diameter and percentages of small and large pores. The threshold diameter of pastes, CP, FAP and SFP exposed to air curing and wet-air curing is presented in Fig. 8 for the various locations considered. The threshold diameter, however, is the diameter before which the pore volume on the cumulative pore volume plot rises sharply. More details about the determination of threshold diameter are given elsewhere [15]. A lower threshold value is indicative of a finer pore size distribution. The trend in the results on the threshold diameter is similar to those obtained in Fig. 2. The largest threshold diameters are obtained for samples taken from the top part of the cube paste, followed by respectively samples taken from the side part, middle part and the

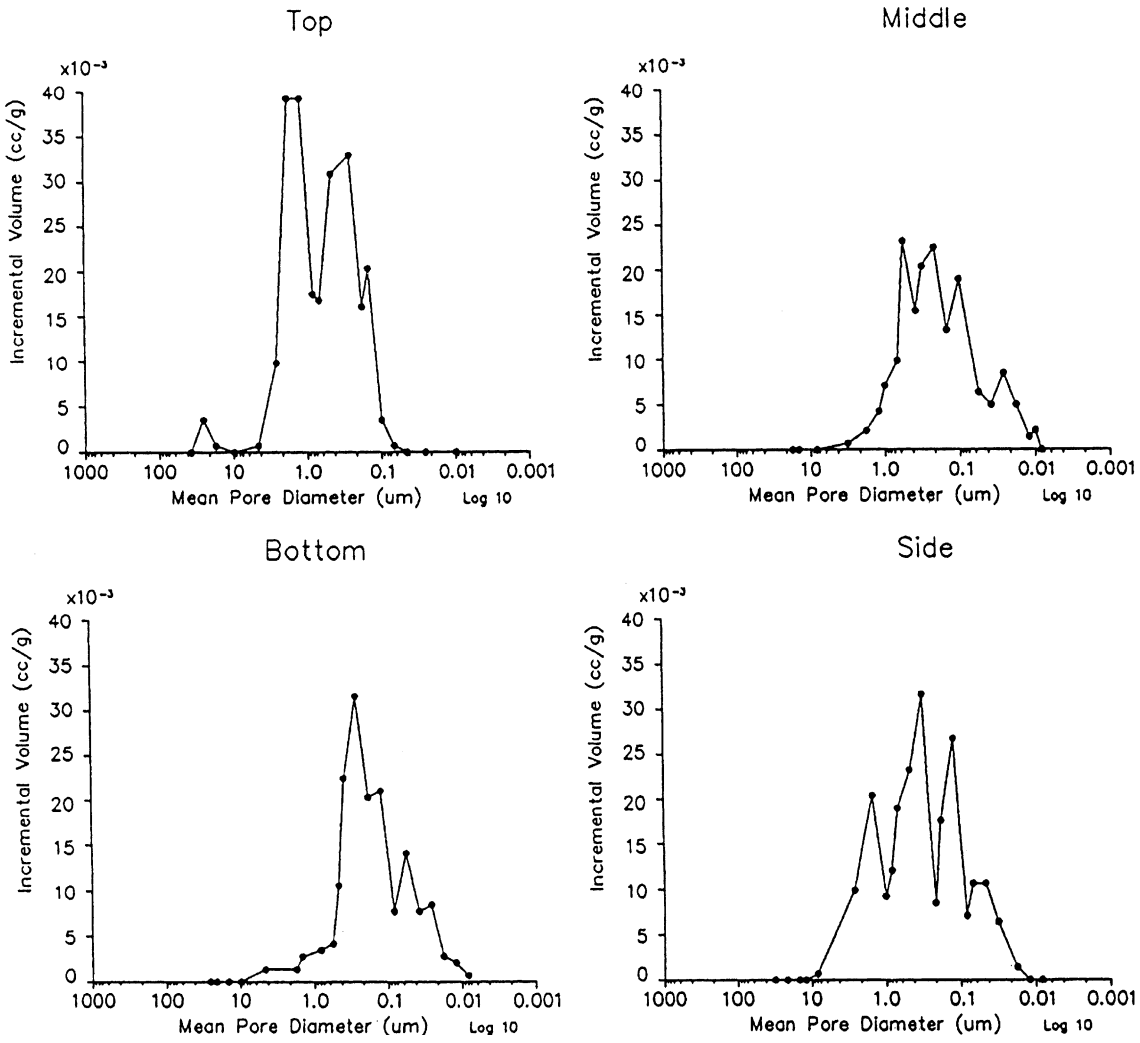

Fig. 4. Influence of position on pore size distribution for the FAP subjected to air curing.

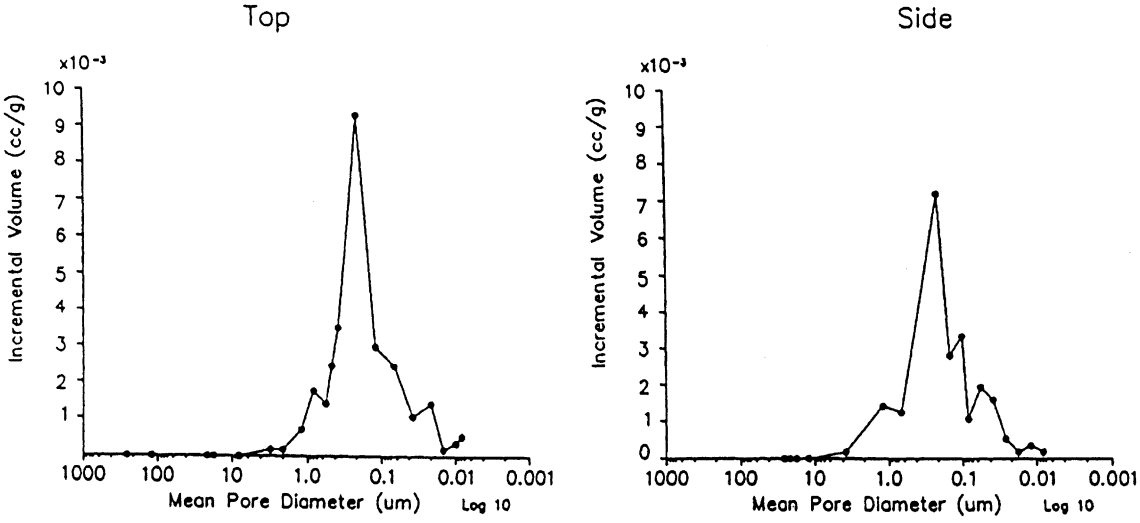

Fig. 5. Influence of position on pore size distribution for the SFP subjected to air curing.

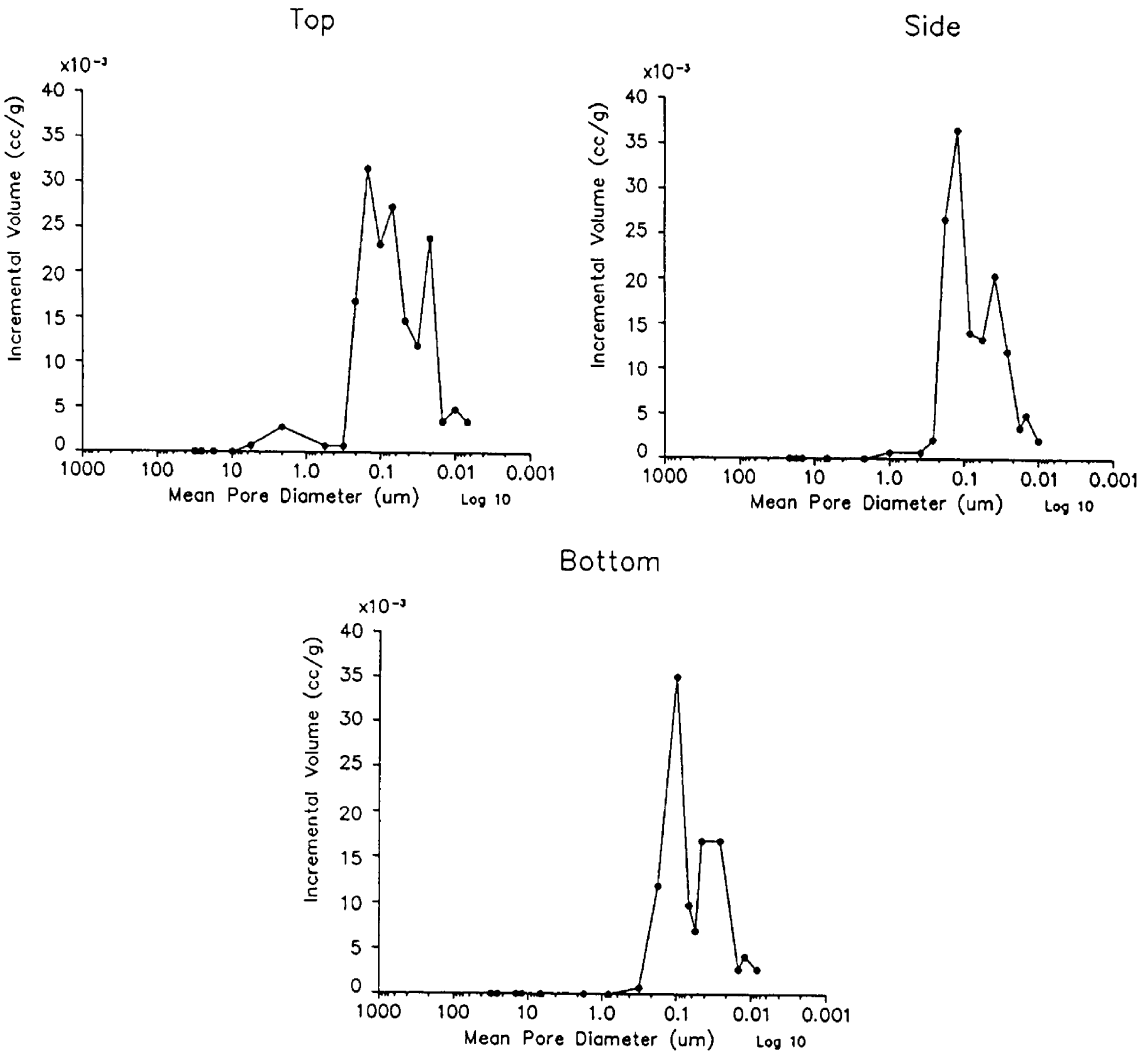

Fig. 6. Influence of position on pore size distribution for the CP subjected to wet-air curing.

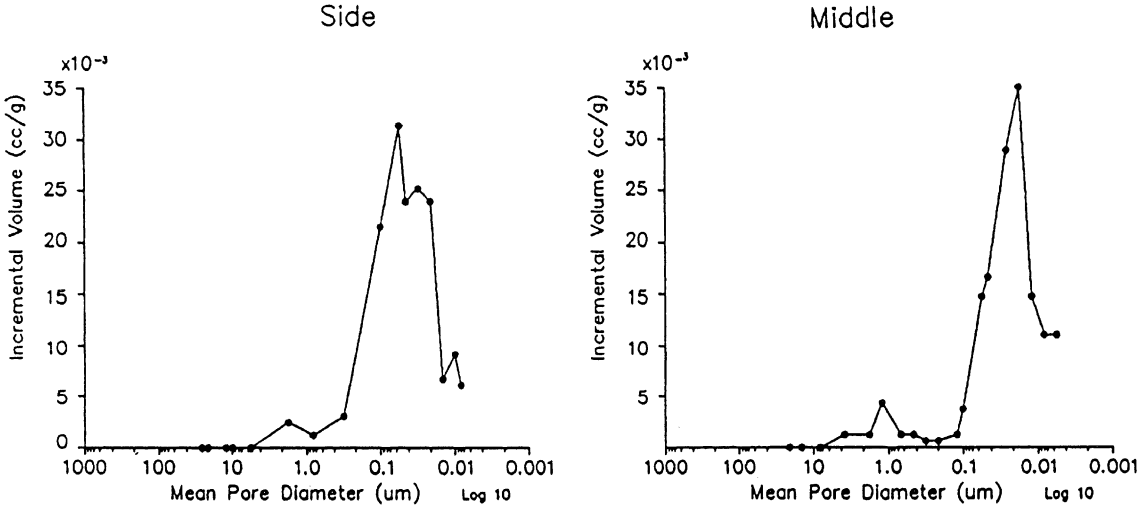

Fig. 7. Influence of position on pore size distribution for the FAP subjected to wet-air curing.

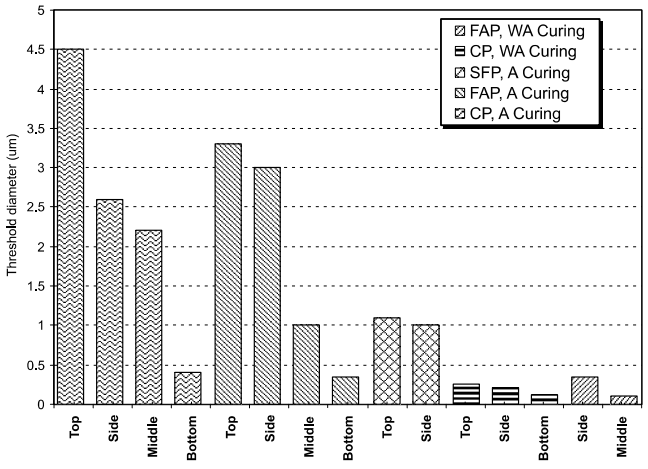

Fig. 8. Influence of location on threshold diameter for the various pastes.

bottom part of the paste. Samples taken from the top, bottom and middle positions of the FAP show lower threshold diameters than the CP. However for the sample taken from the side, the threshold diameter is more than that of the control. The paste containing SF shows a smaller threshold diameter as compared with the CP and the paste containing FA, indicating a smaller pore size distribution in the presence of SF. The threshold diameter is much reduced when specimen is subjected to some initial moist curing as compared to dry curing for all pastes shown in Fig. 8.

The pores in Figs. 3–7 are sub-divided into large pores whose diameter is greater than or equal to 0.1 μm and small pores which have a diameter of less than 0.1 μm. Such division of pores is presented in Table 3 for the various pastes and positions. Samples taken from the top face have the largest proportion of large pores compared to the other positions, followed by the samples taken from the side position. The middle part (core) and the bottom part of specimens showed the least proportion of large pores. The CP, for example, exhibited proportions of large pores of 87.5%, 65.5%, 56.8% and 53.9% for samples taken from the top, side, middle core and bottom positions, respectively. This trend is repeated for the FA blended paste and the SFP subjected to air curing.

When wet-air curing is employed, the percentage of large pores decreased considerably for samples taken from the various location as compared with those subjected to air curing as seen in Table 3. The portions of large pores were 46.4%, 30.9% and 38.7% for the CP, for samples taken from the top, bottom and side positions, respectively. The decrease in the percentages of large pores under wet-air curing is due to the availability of more water during the first 14 days of curing, which allows more hydration to take place, as compared to pastes subjected to air curing. More hydration results in more formation of calcium silicate gel which has a pore blocking effect and therefore, reducing the pore size.

3.3. Bleeding and moisture loss in paste and concrete

The influence of location of sample relative to the casting position on water absoprtion of concrete was reported elsewhere [14]. The concrete mixes were the same as those used in this investigation. The concrete mixes were also cast in 100 mm cube moulds, which is similar to the paste specimens. The initial curing regimes were identical to those for the pastes, except that the total curing period was 90 days instead of 28 days. The

Table 3
Influence of sample location of pastes on large and small pores

Paste	Curing	Position	Pore volume $\times 10^{-2}$ (cc/g)			Pores (%)	
			Total volume	Large pores (>0.1 μm)	Small pores (<0.1 μm)	Large	Small
Control (CP)	A	T	236.2	206.7	29.5	87.5	12.5
		S	178.5	116.8	61.7	65.5	34.5
		MI	139.2	75.1	64.1	53.9	46.1
		B	131.3	74.5	56.7	56.8	43.2
Fly ash (FAP)	A	T	230.8	226.7	4	98.3	1.7
		S	215.2	171.8	43.5	79.9	20.1
		MI	180.3	127	53.3	70.5	29.5
		B	163.1	113.2	49.9	69.4	30.6
Silica fume (SFP)	A	T	283.7	222.4	63.1	78.4	21.6
		S	236.5	164.3	72.3	69.5	30.5
Control (CP)	WA	T	163.5	75.9	87.7	46.4	53.6
		S	135.1	52.3	83	38.7	61.3
		B	106.9	33	73.9	30.9	69.1
Fly ash (FAP)	WA	S	154.5	26.5	128	17.2	82.8
		MI	141.5	14.8	126.8	10.4	89.6

water absorption was conducted on samples having a thickness of about 23 mm and an area of 100 mm × 100 mm cut from 100 mm cubes. Samples were taken from the top part, the bottom part, the middle part and the side part of the cube. Two methods were used to determine the water absorption. The first method was by total immersion in water and the percentage gain in mass as compared with the dry mass was taken to represent the water absorption. The second method was the determination of water absorption by capillarity. This was conducted by placing the face of the sample in contact with water. The amount of water absorbed per unit area was plotted against the square root of time. The initial slope of the line was taken to represent the water absorption coefficient. Further details about casting, curing, sample preparation and testing are given in [14].

In order to compare the influence of location relative to casting position in paste and concrete, the percentage difference in pore volume of the paste and in water absorption of concrete between various locations for specimens exposed to air curing and wet-air curing are presented in Table 4. The bleeding in paste is expected to be more than that of concrete at the same water to binder ratio and for the same thickness of specimen. This would lead to a larger difference between top and bottom position in pore volume of paste as compared to absorption of concrete. Table 4 does not fully support this assumption and the results obtained do not show a clear trend between the variation of location relative to casting position in paste and in concrete, assuming that the intruded pore volume measures the porosity of the paste and absorption by total immersion measures the porosity of the concrete. For example, in the control specimens subjected to air curing, the percentage difference in the pore volume of the paste between the top and bottom part is more than that of water absorption by total immersion of concrete and less than that of absorption by capillary. Water absorption by capillary action, however, is a function of porosity, pore size distribution and the nature of pores (i.e., open or closed pores). Under moist air curing, the control mix do not exhibit similar trend in the percentage difference between the various locations as compared to air cured specimens.

Powers [22] stated that with the normal process of bleeding, water does not rise above the original level of concrete. Therefore, the appearance of a layer of water at the top trowelled face indicates that solids have subsided, leaving the water behind. This is also true in the case of pastes, on which the work was conducted. This layer being thicker in the paste compared to concrete as observed visually.

Subsidence is caused by the gravitational pull of particles, which is opposed by the viscous resistance of water flowing through the space between particles [22]. The bottom layer of the paste is highly compressed compared with the top layer where there is little or no compression. This compression brings the particles closer together and they also fill the voids left by the upward migration of water, which explains the lower pore volume and high percentage of small pores at the bottom layer relative to the top layer.

Also a higher rate of evaporation exists at the top surface for the first 24 h for air cured pastes. The other locations, (bottom, middle and side) lost little or no moisture because the cube specimens remained in the moulds during the first 24 h after casting. The high rate of evaporation at the top surface limits the availability of water for hydration, hence resulting in relatively high porosity.

Samples from the middle part (core) and the side faces are obtained at the same level (Fig. 1), and therefore the degree of sedimentation is similar. The fact that the side positions have a higher pore volume compared to the middle (core) of specimens must, therefore, be due to higher exposure and water evaporation at the surface, especially under dry curing conditions. While

Table 4
Influence of sample location on porosity of paste and concrete

Mix	Curing	Difference between (%)	Paste	Concrete	
			Pore volume	Water absoprtion	Water absoprtion coefficient
Control	A	Top & bottom	44.4	34.9	69.5
		Top & side	24.4	18.4	15.5
		Side & middle	22	3.2	6.2
Fly ash	A	Top & bottom	29.3	49.6	80.7
		Top & side	6.8	31.7	46.7
		Side & middle	16.2	10.7	37.4
Silica fume	A	Top & side	16.6	48.7	77.1
Control	WA	Top & bottom	34.6	40.9	65.4
		Top & side	17.4	23.6	23.4
Fly ash	WA	Side & middle	8.4	1.5	16.8

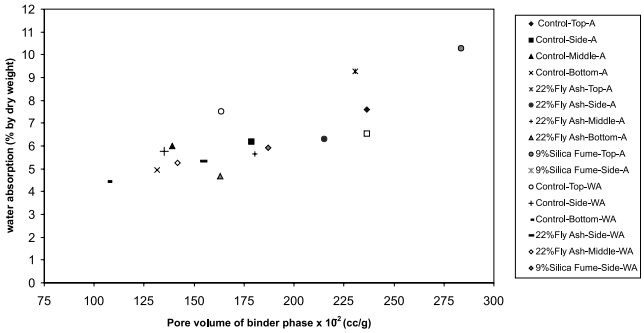

Fig. 9. Relationship between pore volume and water absoprtion.

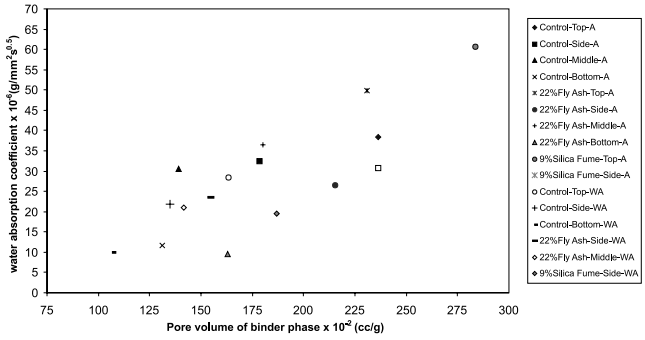

Fig. 10. Relationship between pore volume and water absoprtion coefficient.

evaporation contributes to a coarser pore size distribution, especially at the top, bottom and side faces, the middle position is adequately remote from the surfaces to remain less affected by moisture loss.

3.4. Pore volume, absorption and strength

Fig. 9 shows the relationship between water absorption by total absorption of concrete and pore volume of paste for the various mixes subjected to air and wet-air curing for samples taken from different locations. The water absorption of concrete by capillary action (i.e., water absorption coefficient) vs pore volume of paste, however, is shown in Fig. 10 for the same mixes. As can be expected, an increase in the pore volume of the paste results in an increase in the water absorption of concrete both by total immersion and by capillary rise. The relationship seems to be unaffected by the location of sample relative to casting position. Also the initial curing regime to which a specimen is exposed to and the use of cement replacement material do not influence the relationship. A linear regression analysis yield R^2 values of 0.67 and 0.65 for Figs. 9 and 10, respectively. A better correlation (i.e., a higher correlation coefficient) would be obtained if the interfacial zone between paste and aggregate is taken into consideration. In other words if the intruded volume of the paste is replaced with that of concrete. Unfortunately mercury intrusion porosimetry technique is not suitable for determining the pore volume and pore size distribution of concrete containing large aggregate particles. The use of mortar specimens

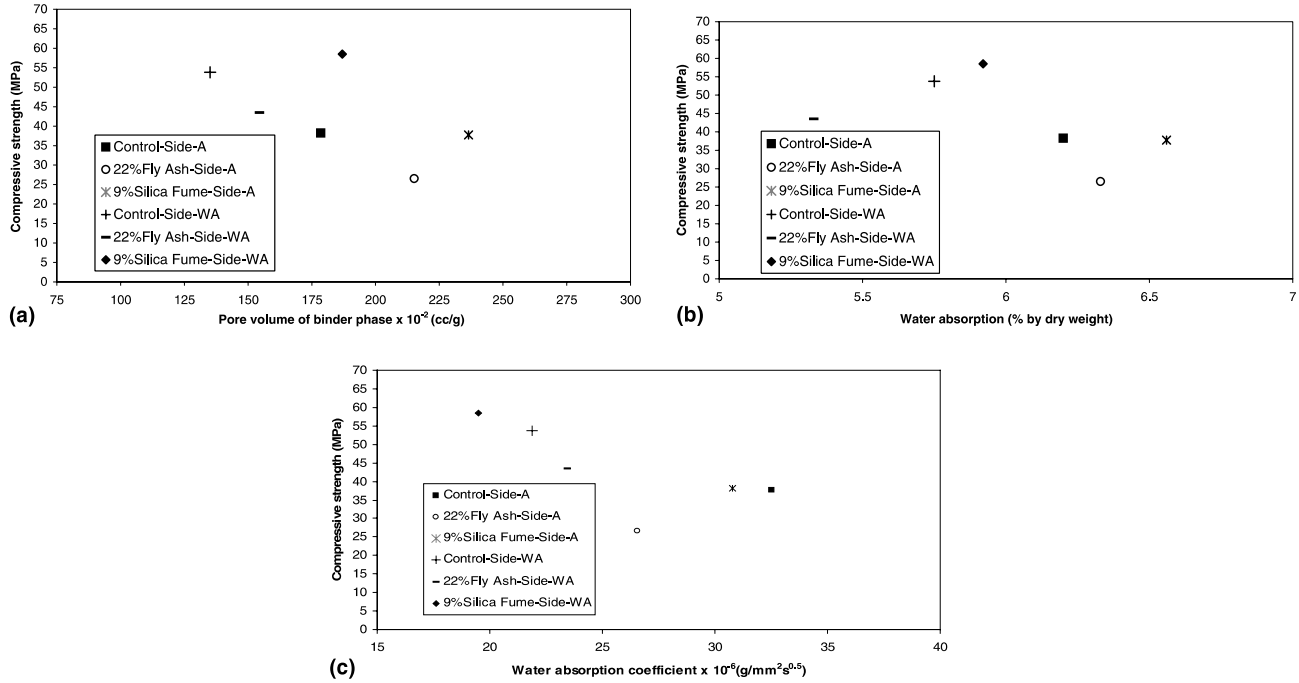

Fig. 11. Relationship between compressive strength vs: (a) pore volume; (b) water absoprtion; (c) water absoprtion coefficient.

can provide better simulation to pore structure than paste. However, this is beyond the scope of the present investigation.

Figs. 11(a)–(c) plots the relationship between cube strength vs respectively the pore volume of paste, the water absorption by total immersion and absorption by capillary action of concrete for samples taken from the side surface. Despite of the limited data available and as can be expected, an increase in the pore volume or absorption results in a decrease in compressive strength.

4. Conclusions

The following conclusions are based on the results of the present investigation:

1. The top surface (trowelled) of a paste possesses larger pore volume than the bottom face. The pore volume near the top surface can be twice as large as the pore volume at the bottom surface.
2. The top surface of a paste has a larger proportion of coarse pores compared with the bottom surface. The proportions of large pores at the top surface under different curing conditions were 87.5%, 98.3%, 82.6% and 46.4% of the total pore volume. The corresponding values at the bottom surface were 65.5%, 79.9%, 70.9% and 38.7%, respectively.
3. The side surface of a paste has a larger pore volume and generally high proportions of large pores compared to that of the middle (core) of a 100 mm cube specimen (i.e., 50 mm from the side surface).
4. Little difference in pore volume and in the percentage volume of large pores exists between the middle core and the bottom surface of a paste specimen.
5. The pore volume and pore size distribution of the top and side faces of a paste are sensitive to curing regimes (temperature and humidity). The middle core (50 mm from the surface) is less sensitive to exposure conditions.

References

[1] Diamond S. A critical comparison of mercury porosimetry and capillary condensation pore size distributions of Portland cement pastes. Cem Concr Res 1971;1(7):531–45.
[2] Manmohan D, Mehta PK. Influence of pozzolanic, slag and chemical admixtures on pore size distribution and permeability of hardened cement paste. Cem Concr Aggregates 1981;3(Summer):63–7.
[3] Sellevold EJ, Bager DH, Klitgaard Jensen E, Knusdsen T. Silica fume-cement pastes: hydration and pore structure, Report BML 82.610. Norwegian Institute of Technology, Trondheim, 1982, p. 19–50.
[4] Cheng-yi H, Feldman RF. Influence of silica fume on the microstructural development in cement mortar. Cem Concr Res 1985;15(2):285–94.
[5] Röbler M, Odler I. Investigations on the relationship between porosity, structure and strength of hydrated cement pastes, I – Effect of porosity. Cem Concr Res 1985;15(2):320–30.
[6] Feldman RF, Cheng-yi H. Influence of silica fume on the microstructural development in cement paste. Cem Concr Res 1985;15(2):285–94.
[7] Kumar A, Roy DM. Pore structure and ionic diffusion in admixture blended Portland cement systems. In: Proceedings of the 8th International Conference on the Chemistry of Cement, Rio de Janeiro, vol. V. 1986. p. 73–9.
[8] Reinhardt HW, Gaber K. From pore size distribution to an equivalent pore size of cement mortar. Mater Struct (RILEM) 1990;23(2):3–15.
[9] Winslow DN, Liu D. The pore structure of paste in concrete. Cem Concr Res 1990;20(2):227–35.
[10] Mangat PS, El-Khatib JM. Influence of initial curing on pore size distribution and porosity of blended cement concrete. In: Malhotra VM, editor. 4th International Conference on Fly Ash, Slag and Natural Pozzolans in Concrete, SP 132, vol. 1. American Concrete Institute; 1992. p. 813–33.
[11] Diamond S, Bonen D. Microstructure of hardened cement paste – A new interpretation. J Am Ceram Soc 1993;75(12):2993–9.
[12] Ramezanianpour AA, Malhotra VM. Effect of curing on the compressive strength. Resistance to choloride-ion penetration and porosity of concretes incorporating slag, fly ash or silica fume. Cem Concr Compos 1995;17:125–33.
[13] Wee TH, Matsunaga Y, Watanable Y, Sakai E. Microstructure and strength properties of high strength concretes containing various mineral admixtures. Cem Concr Res 1995;25(4):715–20.
[14] Khatib JM, Mangat PS. Absorption characteristics as a function of location in the concrete matrix. Cem Concr Res 1995;25(5):999–1010.
[15] Khatib JM, Wild S. Pore size distribution of metakaolin paste. Cem Concr Res 1996;26(10):1545–53.
[16] Shi C. Strength, pore structure and permeability of alkali-activated slag mortars. Cem Concr Res 1996;26(12):1789–99.
[17] Takahashi T, Yamamoto M, Ioku K, Goto S. Relationship between compressive strength and pore structure of hardened cement pastes. Adv Cem Res 1997;9(33):25–30.
[18] Poon CS, Wong YL, Lam L. The influence of different curing conditions on the pore structure and related properties of fly-ash cement pastes and mortars. Constr Building Mater 1997;11(7–8):383–93.
[19] Jiang L, Guan Y. Pore structure and its effect on strength of high-volume fly ash paste. Cem Concr Res 1999;29(5):633–5.
[20] Cook RA, Hover KC. Mercury porosimetry of hardened cement pastes. Cem Concr Res 1999;29(7):933–43.
[21] Pandey SP, Sharma RL. The influence of mineral additives on the strength and porosity of OPC mortar. Cem Concr Res 2000;30(1): 19–23.
[22] Powers TC. The bleeding of Portland cement paste and mortar and concrete. Bull Res Lab Portland Cem Assoc 1939;2.
[23] Senbetta E, Scholer CF. A new approach for testing concrete curing efficiency. ACI J 1984;81(January–February): 82–6.
[24] Wainwright PJ, Rey N. The influence of ground granulated blastfurnace slag (GGBS) additions and time delay on the bleeding of concrete. Cem Concr Compos 2000;22(2):253–7.
[25] Giaccio G, Giovambattista A. Bleeding: evaluation of its effects on concrete behaviour. Mater Struct (RILEM) 1986;112:265–71.
[26] Berry EE, Malhotra VM. Fly ash for use in concrete – a critical review. Am Concr Inst J 1980;(March–April):59–73.
[27] Parker GD. Microsilica concrete. Part 1: The material. Concrete 1985;(October):21–2.

[28] Frias M, Sanchez de Rojas MI. Microstructural alterations in fly ash mortar: study on phenomena affecting particle and pore size. Cem Concr Res 1997;27:619–28.
[29] Hassan KE, Cabrera JG, Maliehe RS. The effect of mineral admixtures on the properties of high-performance concrete. Cem Concr Compos 2000;2:267–71.
[30] Mangat PS, El-Khatib JM. Influence of initial curing on sulphate resistance of blended cement concrete. Cem Concr Res 1992;22: 1089–100.
[31] Washburn EW. Note on method of determining the distribution of pore sizes in porous materials. In: Proceeding of the National Academy of Science, USA, vol. 7. 1921. p. 115–6.